applied sciences

MDPI

Article

Performance of a High-Speed Pyroelectric Receiver as Cryogen-Free Detector for Terahertz Absorption Spectroscopy Measurements

Jente R. Wubs [1], Uwe Macherius [1], Xiang Lü [2], Lutz Schrottke [2], Matthias Budden [3], Johannes Kunsch [4], Klaus-Dieter Weltmann [1] and Jean-Pierre H. van Helden [1,*]

[1] Leibniz Institute for Plasma Science and Technology (INP), Felix-Hausdorff-Str. 2, 17489 Greifswald, Germany; jente.wubs@inp-greifswald.de (J.R.W.); macherius@inp-greifswald.de (U.M.); weltmann@inp-greifswald.de (K.-D.W.)
[2] Paul-Drude-Institut für Festkörperelektronik, Leibniz-Institut im Forschungsverbund Berlin e. V., Hausvogteiplatz 5–7, 10117 Berlin, Germany; lue@pdi-berlin.de (X.L.); lutz@pdi-berlin.de (L.S.)
[3] WiredSense GmbH, Luruper Hauptstr. 1, 22547 Hamburg, Germany; matthias.budden@wiredsense.com
[4] Laser Components Germany GmbH, Werner-von-Siemens-Str. 15, 82140 Olching, Germany; j.kunsch@lasercomponents.com
* Correspondence: jean-pierre.vanhelden@inp-greifswald.de

Abstract: The application of terahertz (THz) radiation in scientific research as well as in applied and commercial technology has expanded rapidly in recent years. One example is the progress in high-resolution THz spectroscopy based on quantum cascade lasers, which has enabled new observations in astronomy, atmospheric research, and plasma diagnostics. However, the lack of easy-to-use and miniaturised detectors has hampered the development of compact THz spectroscopy systems out of the laboratory environment. In this paper, we introduce a new high-speed pyroelectric receiver as a cryogen-free detector for THz absorption spectroscopy. Its performance is characterised by absorption spectroscopy measurements on a reference gas cell (RGC) with ammonia using a tunable THz quantum cascade laser at approximately 4.75 THz as the light source. It is shown that the receiver can record spectra up to 281 Hz without any artefacts to the observed spectral absorption profile, and the results reproduce the known pressure of ammonia in the RGC. This demonstrates that the pyroelectric receiver can be reliably used as an alternative to helium-cooled bolometers for absorption spectroscopy measurements in the THz range, with its main advantages being the high bandwidth, compactness, relatively low cost, and room-temperature operation. Its simplicity and high sensitivity make this receiver a key component for compact THz spectroscopy systems.

Keywords: terahertz; spectroscopy; pyroelectric receiver; quantum cascade laser

Citation: Wubs, J.R.; Macherius, U.; Lü, X.; Schrottke, L.; Budden, M.; Kunsch, J.; Weltmann, K.-D.; van Helden, J.-P.H. Performance of a High-Speed Pyroelectric Receiver as Cryogen-Free Detector for Terahertz Absorption Spectroscopy Measurements. *Appl. Sci.* **2024**, *14*, 3967. https://doi.org/10.3390/app14103967

Academic Editor: Mira Naftaly

Received: 9 April 2024
Revised: 24 April 2024
Accepted: 3 May 2024
Published: 7 May 2024

Correction Statement: This article has been republished with a minor change. The change does not affect the scientific content of the article and further details are available within the backmatter of the website version of this article.

1. Introduction

For a long time, the electromagnetic radiation in the terahertz (THz) spectral region from microwaves to the far infrared (100 GHz–30 THz) was known as the so-called THz gap due to the lack of suitable radiation sources and detectors in this spectral range. During the last three decades, however, this has changed as the related technology has advanced, and the emerging technology has started to leave the laboratory environment, leading to commercial applications. As a result, the field of THz technology has continued to develop and expand rapidly. Despite this progress, many challenges remain in the field of THz science and technology [1–3]. Among some of the most promising THz sources for high-resolution absorption spectroscopy are quantum cascade lasers (QCLs). The first QCL with an emission frequency in the THz range was reported in 2002 by Köhler et al. [4]. THz QCLs cover, at present, the emission frequency range of about 1 THz to 5.5 THz [5–7]. In this spectral region, QCLs are the only available powerful cw radiation sources, with optical output powers of up to a few mW and extremely narrow linewidths of a few MHz

down to kHz. The applicability of THz QCLs has already been demonstrated for numerous applications, such as THz real-time imaging [8,9], THz sensing [10], and microscopy [11]. Another emerging application is the use of THz QCLs for high-resolution spectroscopy, since many transitions of atoms and molecules can be accessed, enabling selective and sensitive spectroscopic measurements of a large number of compounds. In particular, the detection of fine structure transitions in atoms is of high interest, as this could provide a means of developing absolute detection methods for atoms based on direct absorption spectroscopy. Recent examples of this are the detection of atomic oxygen by heterodyne spectroscopy in astronomy and atmospheric research [12–14] and the determination of the absolute densities of oxygen atoms in a plasma reactor [15–17]. There have been a few reports on the application of THz QCLs for absorption spectroscopy in the gas phase as well [18–21].

However, the lack of suitable and miniaturised detectors has hampered the development of compact THz spectroscopy systems out of the laboratory environment as often helium-cooled bolometers or Ge:Ga photoconductive detectors are used as detectors. In addition to the requirement of cryogenic cooling, they typically have a limited bandwidth in the order of up to a few hundred Hz for the 3 dB roll-off frequency, which significantly reduces the laser tuning frequencies that can be applied and thus leads to longer measurement times when recording an absorption spectrum. For example, in previous work [15,16], laser tuning frequencies of 10 Hz or 11 Hz had to be used to avoid any asymmetric deformation of the observed absorption features, which, in turn, also limited the spectral range that could be probed.

Pyroelectrics are another type of thermal detector based on direct energy detection and have long been used to measure infrared and THz radiation. So far, however, it has been reported that pyroelectrics typically work at low speed and with relatively low sensitivity. In addition, microphonics is a problem that significantly increases the detector noise.

This paper reports on the performance of a new high-speed pyroelectric receiver as a cryogen-free detector for THz absorption spectroscopy measurements. The novelty of the reported work is twofold. Firstly, it will be demonstrated that an absorption spectroscopy experiment in the THz range can be performed with an uncooled detector, for which the signal-to-noise ratio (SNR) of the recorded absorption spectra with the same measurement time is only a factor of 2 lower than measurements performed with a helium-cooled bolometer. Secondly, it is shown that this can be achieved by $LiTaO_3$-based pyroelectric detector technology, whereas previous work was in favour of DLaTGS detectors (deuterated L-alanine-doped triglycene sulphate) [22]. The choice of $LiTaO_3$ is supported by the work of Whatmore et al. [23], who calculated that $LiTaO_3$ does outperform DLaTGS in terms of the integrated detectivity from 100 Hz to 1 kHz. Furthermore, the $LiTaO_3$-based pyroelectric detector used in this work does not require active temperature stabilisation, in contrast to DLaTGS-based pyroelectric detectors, which should be actively temperature stabilised when used in metrology [22].

In this paper, we first describe in detail some of the relevant detector characteristics, such as the frequency-dependent sensitivity, noise, and detectivity. This is followed by a comprehensive analysis of the absorption spectroscopy measurements. The measurements were carried out on a gas cell filled with ammonia gas (NH_3) using a tunable THz QCL at approximately 4.75 THz as the light source. The results are compared to those obtained with a bolometer to demonstrate that the pyroelectric receiver can be used as an alternative to helium-cooled bolometers for fast and accurate absorption spectroscopy measurements in the THz range.

2. Materials and Methods

For this work, the uncooled pyroelectric receiver PR No1 THz (Laser Components) was used. While it is a state-of-the-art $LiTaO_3$-based receiver, it incorporates a redesign of all core components: the detector element (see Figure 1a) and the amplifier electronics. The goal was to increase both speed and detectivity to enable undistorted broadband measurements of

typical infrared signals down to 0.5 THz. Until now, pyroelectric detectors in spectroscopy, especially in Fourier-transform infrared (FTIR) spectroscopy, have mostly been operated in voltage mode. The PR No1 exploits a proprietary current mode configuration that is specifically tailored to the pyroelectric sensor elements. When radiation is absorbed by the black coating of the pyroelectric detector element, it causes a slight increase in its temperature. This, in turn, leads to a charge separation at the detector interfaces. The resulting current is amplified and converted into a voltage by a transimpedance amplifier. A simplified schematic circuit of this so-called current mode operation is shown in Figure 1b, where D_{py} indicates the pyroelectric detector element. The proprietary amplifier electronics of the PR No1 are optimised to provide a high gain at a very low noise level while still offering an electronic bandwidth of 8 kHz. In particular, the electronics are low-noise even for current sources with a high capacity, which is typical for thin and fast pyroelectric detector elements.

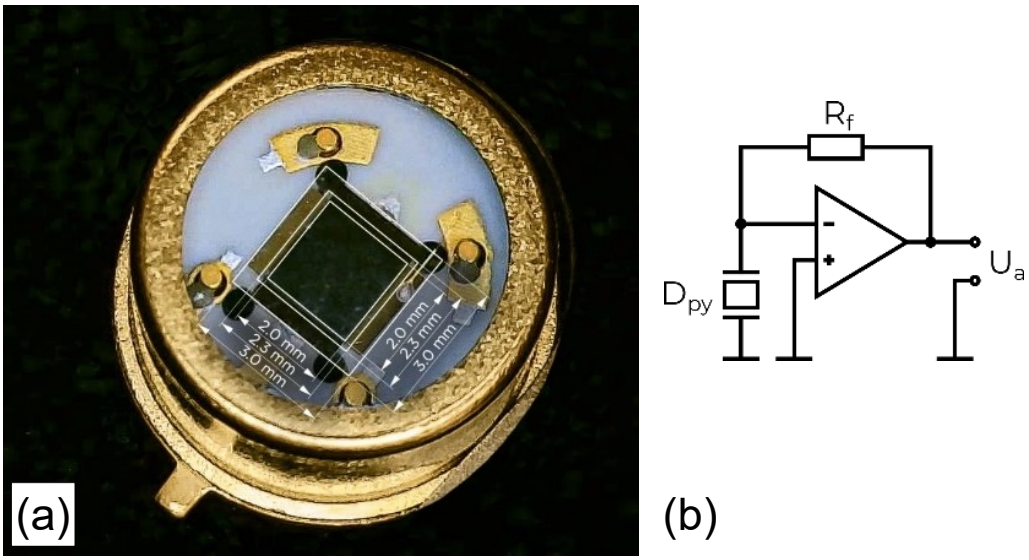

Figure 1. (**a**) A photograph (30× magnification) of the $LiTaO_3$ chip mounted on a header. A thin membrane (2.3 × 2.3 mm^2, 6 µm thickness) is etched into a frame (3.0 × 3.0 mm^2, 20 µm thickness) and then coated (2.0 × 2.0 mm^2). Vibration dampening is achieved by 4 flexible posts. All wire bonds have been made on the frame. The element is sealed by a TO-can assembly with an HDPE window (0.8 mm thickness). (**b**) A simplified schematic circuit of the current mode configuration.

The improved receiver technology enables high internal amplification and thus high responsivity of up to 70 kV/W at low noise density (down to 25 µV/$\sqrt{\text{Hz}}$), resulting in a high detectivity of up to 4×10^8 cm $\sqrt{\text{Hz}}$/W. At the same time, the receiver's 3 dB bandwidth of 8 kHz is much higher than the one of common pyroelectric detectors in voltage mode (typically 10–100 Hz). Up to the 3 dB bandwidth, the receiver is able to measure undistorted signals with a linearity of 1% or better over 4 decades in power. This characteristic is particularly important for this work. Furthermore, the spatial uniformity over the 2 × 2 mm^2 active detector area is better than 10%. $LiTaO_3$ was chosen as basic detector material because of its ruggedness. No cooling is required, and all measurements in this work were performed at room temperature. The detector window was made from thin high-density polyethylene (HDPE) for good transmission in the far infrared.

The absorption spectroscopy measurements were performed on a reference gas cell (RGC) filled with ammonia gas to a precisely known pressure. A tunable, continuous-wave (cw) THz QCL with an output power of approximately 4 mW was used as the THz source [7]. The same THz QCL has been used in previous work to detect the $^3P_1 \leftarrow {}^3P_2$ fine structure transition of ground-state atomic oxygen at approximately 4.75 THz, which corresponds to approximately 158 cm^{-1} and a wavelength of approximately 63.2 µm [15,16]. The QCL was operated in a Stirling cryocooler (Ricor K535) at a temperature of 43.3 K while

temperature fluctuations were minimised to be below 5 mK by an additional temperature controller (Stanford Research Systems, Sunnyvale, CA, USA, CTC100). Tuning of the laser output was performed by linearly ramping the input current. To this end, a current with a sawtooth waveform was supplied by a laser driver (Wavelength Electronics, Bozeman, MT, USA, QCL1000 OEM) controlled by a function generator (Tektronix, Beaverton, OR, USA, AFG3022C). Continuous ramping instead of discrete stepping of the current was possible due to the stable and mode-hop-free behaviour of the used THz QCL, allowing for fast measurements with high spectral resolution. The spectral resolution was given by the laser linewidth and was equal to approximately 2×10^{-4} cm^{-1}, i.e., approximately 6 MHz. The repetition frequency of the sawtooth current waveform is the so-called laser tuning frequency. In previous works [15,16], laser tuning frequencies of 10 Hz or 11 Hz were used; however, faster measurements were hampered by the limited bandwidth of the used bolometer (Infrared Laboratories, Tucson, AZ, USA, 4.2K Bolometer; 3 dB roll-off frequency of 500 Hz), leading to an asymmetric deformation of the observed absorption features [15]. The larger bandwidth of the pyroelectric receiver (Laser Components Germany, Olching, Germany, PR No1; 3 dB roll-off frequency of 8 kHz) should allow to increase the laser tuning frequency without causing a deformation of absorption features. To investigate the detector performance for different frequencies, the laser tuning frequency was varied from 11 Hz to 4 kHz.

The laser beam with a full width at half maximum (FWHM) of approximately 3 mm was focused on the detector element by a gold-coated off-axis parabolic mirror (OAP). The OAP was positioned such that removing it led to the laser beam being incident on the bolometer. This is schematically visualised in Figure 2a. A photograph of the two detectors is included in Figure 2b, demonstrating their difference in size, which is one of the advantages of the pyroelectric receiver with respect to the bolometer. As indicated in Figure 2a, a major part of the laser beam path could be purged with nitrogen gas to minimise the absorption by atmospheric water vapour. Since only temperature changes can be detected, the laser output was modulated by a phase-locked optical chopper (New Focus, San Jose, CA, USA, Model 3502) with a modulation frequency equal to half the laser tuning frequency, such that each second period of the laser output was blocked by the optical chopper. Although the investigated absorption features could still be observed without modulating the laser beam, the use of a chopper was essential to determine the baseline, this being a crucial requirement for quantitatively analysing the absorption features. As a consequence of the limited speed of the used chopper, determining the density of NH_3 from measured absorption spectra was possible for tuning frequencies of maximally 281 Hz. The detected signals were recorded with a digital sampling oscilloscope (R&S, Munich, Germany, RTO 1014), and all results presented in this paper were averaged over 2000 single measurements to improve the SNR.

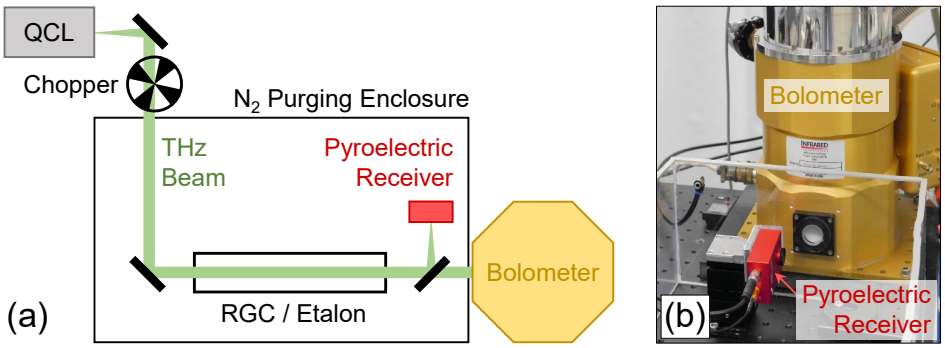

Figure 2. (**a**) A schematic overview (not to scale) of the THz beam path from QCL to detector (green) with either the pyroelectric receiver (red) or the bolometer (yellow) as detector, and (**b**) a photograph showing both detectors.

3. Results and Discussion

3.1. Characterisation of Detector Properties

The detector response curve in Figure 3a was measured by varying the frequency of a pulsed laser diode from 10 Hz to 100 kHz while the receiver signal was acquired with an oscilloscope (Red Pitaya, Solkan, Slovenia, STEMlab 125–14). A power-calibrated laser at 1.55 µm wavelength with a custom-built driver, a duty cycle of 50%, and 1 mW of average laser power was used for this measurement. To obtain an absolute calibration of the response data in units of V/W, the level of the first harmonic of the detector response was measured at a fixed distance with a calibrated black-body emitter (Dias Infrared, Dresden, Germany, Pyrotherm CS F150) at 150 °C with a wavelength peak emission at 6.8 µm in combination with an optical chopper at 139 Hz. For given detector dimensions and distances to the black-body emitter, the absolute power levels reaching the detector element were calculated and used to calibrate the frequency-resolved response curve. It should be noted that the measured frequency–responsivity, as indicated by the blue curve in Figure 3a, deviated from the intrinsic detector responsivity due to the presence of the HDPE window. Calculating the intrinsic detector responsivity by taking into account the transmission losses of the window (transmission of 26.7% at a wavelength of 6.8 µm) led to higher responsivity values, as given by the green curve in Figure 3a.

The noise spectral density of the detector (see Figure 3b) was measured with a fast Fourier-transform analyser (Ono Sokki, Yokohama, Japan, CF-5220) from 10 Hz to 100 kHz. The frequency-resolved detectivity (D*) (see Figure 3c) was calculated from both the calibrated response and the noise density.

3.2. THz Absorption Spectroscopy Measurements

First, etalon measurements were performed for different laser tuning frequencies to investigate the current–wavenumber relation and its possible dependence on the tuning frequency. Examples of etalon measurements for tuning frequencies of 11 Hz and 201 Hz are shown in Figure 4. The used etalon was made of silicon (refractive index: $n = 3.4175 \pm 0.003$ [24]) and had a length L of 9 cm. The low transmission of this etalon led to very weak signals with fringes that were hardly discernable due to the poor SNR, even after averaging. Hence, the data were filtered with a Savitzky–Golay filter before determining the positions of the minima and maxima of the fringes. As can be seen from Figure 4, the minima and maxima occurred at the same wavenumber position independent of the laser tuning frequency. The distance in wavenumber between the fringes is given by $1/(2nL)$ and equal to 0.016 cm^{-1}, resulting in a tuning coefficient of 7.8×10^{-4} cm^{-1}/mA. This value is in good agreement with results of previous measurements performed with a bolometer as the THz detector [15,16]. The same value for the tuning coefficient was obtained for various laser tuning frequencies up to 281 Hz. Therefore, it can be concluded that the tuning behaviour of the used THz QCL is not affected by the tuning frequency, at least not for tuning frequencies up to 281 Hz (for a temperature of 43.3 K and laser currents between 480 mA and 600 mA).

This also confirms that the same tuning coefficient can be used when lowering the tuning speed by reducing the tuning range, which was a critical assumption for previous bolometer-based measurements as the tuning range needed for etalon measurements typically involved tuning speeds that proved too fast to accurately detect the shape of sharp absorption features [15].

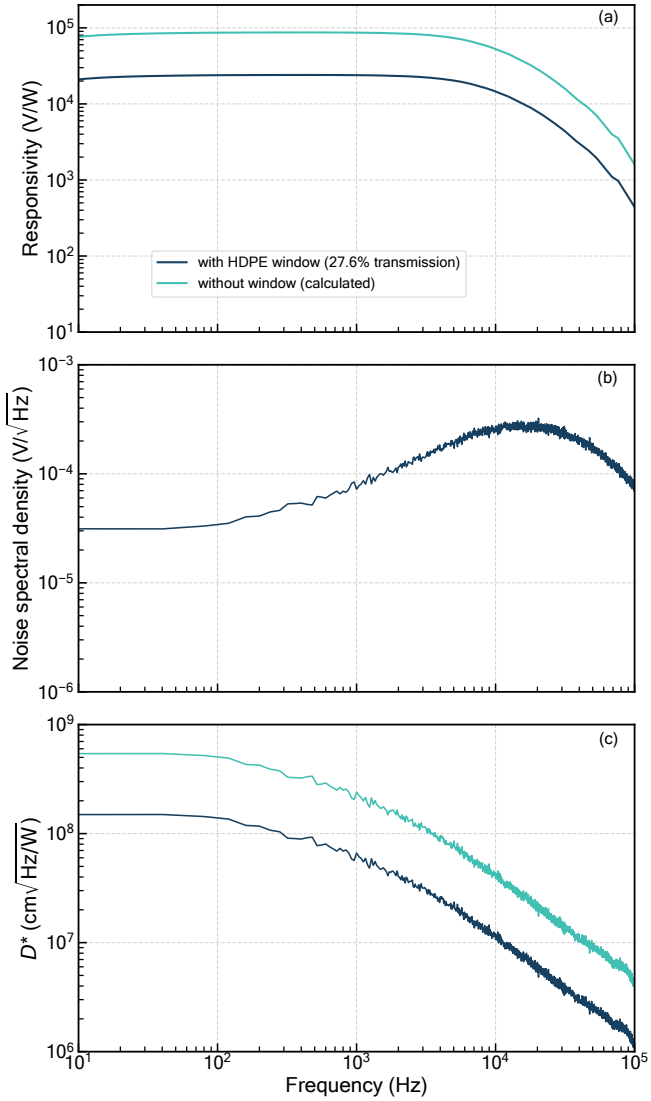

Figure 3. (**a**) Frequency-resolved responsivity, (**b**) noise spectral density, and (**c**) detectivity (D*) of the PR No1 pyroelectric receiver. The responsivity and D* values were measured with a 150 °C black-body emitter with 6.8 µm peak emission. The blue curves are raw measurement data while the green curves were calculated from these data to compensate for the transmission losses of HDPE at the wavelength of 6.8 µm.

Next, measurements were performed on an RGC with NH_3. The cell had a length L of 15 cm and silicon windows at both ends which were attached under an angle to avoid an etalon effect between the parallel window surfaces. It was filled with pure NH_3 to a precisely known pressure of (1.61 ± 0.01) mbar, determined using frequency-comb-based Fourier-transform spectroscopy in the range from 3145 cm^{-1} to 3390 cm^{-1} [25]. Figure 5a shows the raw results of measurements on this gas cell for laser tuning frequencies of 11 Hz and 201 Hz using the same tuning range (480 mA to 600 mA) as for the etalon measurements. Two absorption features can be observed, of which the more prominent one located at approximately 580 mA was identified as the R(7,5)-transition of $^{15}NH_3$ at 158.257314 cm^{-1} [26,27]. The smaller absorption feature at approximately 530 mA was due to the aR(7,2)-transition of $^{14}NH_3$ at 158.2958 cm^{-1} [15,27,28]. The assignment notation used here corresponds to $\Delta J(J'', K_a'')$, where J'' and K_a'' are the lower-state quantum numbers of the $(J', K_a') \leftarrow (J'', K_a'')$ transition, J is associated with the total angular momentum, and K_a with its projection along the principle axis (C3) of the ammonia molecule. Notably, both absorption features were recorded without significant deformations, even for a tuning

frequency of 201 Hz, whereas the same absorption features measured with a bolometer were already asymmetrically deformed for a tuning frequency of 10 Hz [15]. A reduction in the laser tuning range from 120 mA to 10 mA or 20 mA was necessary to avoid this unwanted effect. Using the pyroelectric receiver with a similar laser tuning range, asymmetric deformations started to appear for laser tuning frequencies of approximately 1 kHz or higher. However, such high frequencies were above the maximum speed of the used chopper; therefore, only the shape of detected absorption spectra could be studied, and a faster chopper would be required for a quantitative analysis.

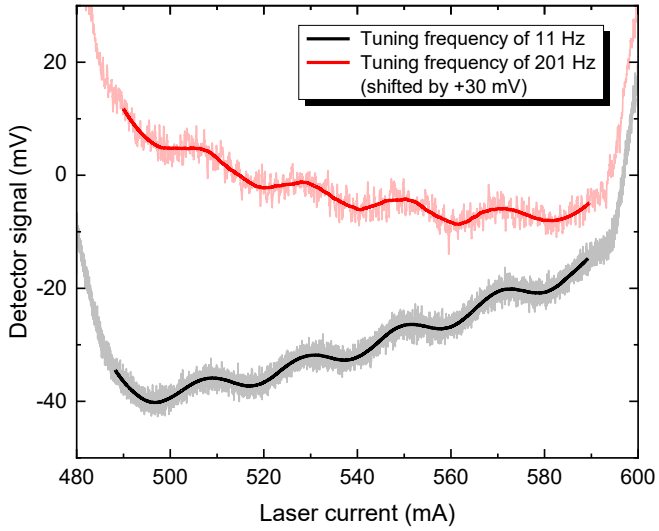

Figure 4. Etalon measurements for different laser tuning frequencies (Si etalon with a length of 9 cm). The measured data are averaged over 2000 single measurements and have been smoothed with a Savitzky–Golay filter. The data for 201 Hz are vertically shifted by +30 mV for a better comparison.

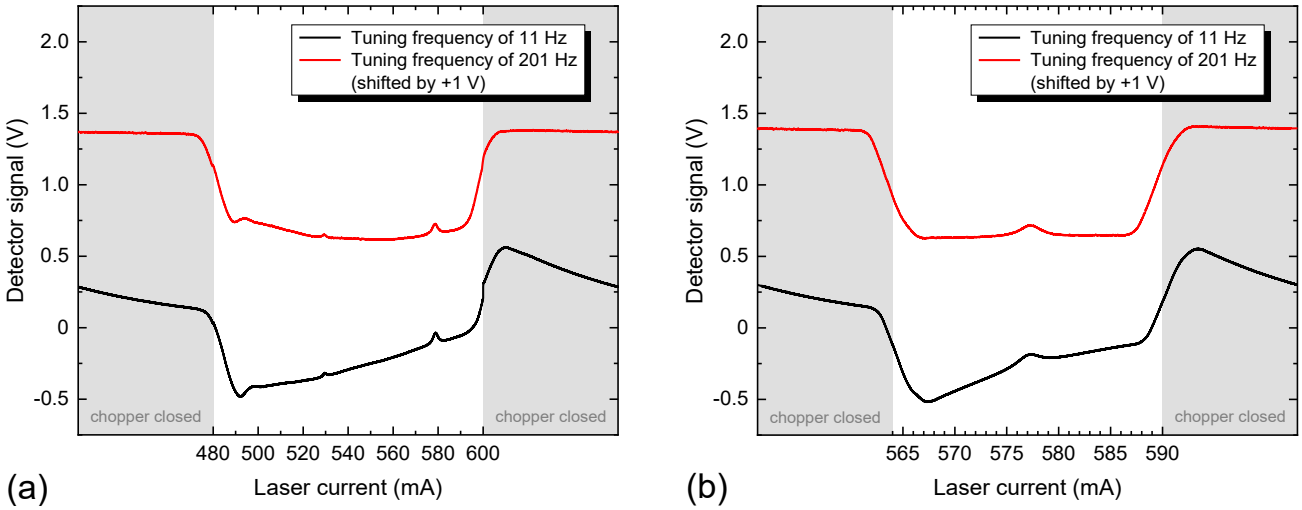

Figure 5. Measurements on an RGC with NH_3 (pressure of 1.6 mbar, length of 15 cm) for different laser tuning frequencies using (**a**) a tuning range of 480 mA to 600 mA and (**b**) a tuning range of 564 mA to 590 mA. The measured data are averaged over 2000 single measurements. The data for 201 Hz are vertically shifted by +1 V for a better comparison.

Figure 5b shows the absorption feature corresponding to the R(7,5)-transition of $^{15}NH_3$, recorded using a narrower tuning range of 564 mA to 590 mA for accurate analysis of this individual absorption feature. The major difference between measurements taken at 11 Hz and 201 Hz is constituted by the baseline, i.e., the line corresponding to zero intensity detected. Naturally, it can only be measured for the time period during which the

chopper is closed, based on which an estimation of the baseline has to be made for when the chopper is open. From Figure 5a,b, it can be seen that the baseline can be approximated by a flat horizontal line when using a laser tuning frequency of 201 Hz, whereas it is more sloping and possibly nonlinear when using a laser tuning frequency of 11 Hz. Note that the black and red curves shown in Figure 5a as well as those shown in Figure 5b should have the same shape after subtracting the baseline, i.e., the increase in the detector voltage with increasing laser current observed for a laser tuning frequency of 11 Hz is purely a consequence of the increasing trend of the baseline voltage. Correctly determining the baseline is critical; however, estimating the baseline without knowing its shape is prone to errors, thus complicating an accurate determination of the NH_3 density and the pressure in the cell. Therefore, the pyroelectric receiver is best suited for absorption spectroscopy measurements when used in combination with laser tuning frequencies of 201 Hz or higher.

The raw spectrum shown in Figure 5b was analysed by calculating the absorbance as follows:

$$\text{Absorbance} = -\ln\left(I/I_0\right), \tag{1}$$

where I is the measured intensity with respect to the baseline and I_0 the intensity that would have been measured without absorption. The shape of I_0 was predominantly determined by the spectral laser power and the absorption due to atmospheric water vapour, in particular, the far-reaching wings of the absorption line of H_2O at approximately 157.9 cm^{-1} [27]. Because of noise and fluctuations, I_0 could not be measured separately, and it was estimated by fitting a linear function to I (i.e., the part for which the chopper was fully opened) while excluding the part affected by absorption from the fit (i.e., the range from -0.0053 cm^{-1} to $+0.0053$ cm^{-1} with respect to the central line position). The resulting absorption spectrum is shown in Figure 6. It was fitted with a Voigt function and the corresponding residual, i.e., the difference between the measured absorption profile and the fit, included in Figure 6 as well. Notably, it has no pronounced W shape, especially when compared to the previous measurements with a bolometer [15,16].

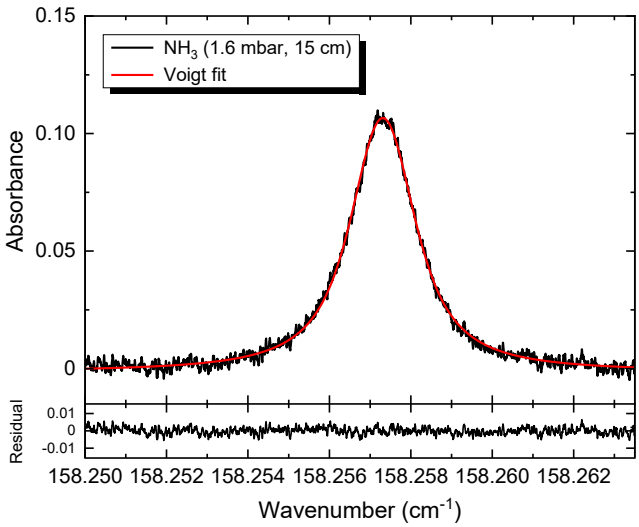

Figure 6. Spectral absorption profile of the R(7,5)-transition of $^{15}NH_3$ at 158.257314 cm^{-1}, measured in an RGC with NH_3 (pressure of 1.6 mbar, length of 15 cm) using a laser tuning frequency of 201 Hz and a tuning range of 564 mA to 590 mA. The measured data are averaged over 2000 single measurements. A Voigt fit was fitted to the profile; the corresponding residual is given in the bottom part of the figure.

According to the Lambert–Beer law, the area under the absorption profile is directly proportional to the density of NH_3 and given by

$$\int_{\text{line}} \text{Absorbance}(\nu)\, \mathrm{d}\nu = n_{NH_3}\, L\, S(T), \tag{2}$$

where L is the absorption length, $S(T)$ the line strength of the investigated absorption transition [26,27], and n_{NH_3} the density of NH_3, which is related to the pressure p by the ideal gas law ($p = n_{NH_3} k_B T$, with $T = 296$ K). Following this, the pressure inside the gas cell was determined from the absorption spectrum shown in Figure 6, resulting in (1.65 ± 0.10) mbar. A similar value was obtained after analysing the measurements with the broader tuning range of 480 mA to 600 mA, i.e., the red curve in Figure 5a. The indicated possible error of approximately 6% accounts for uncertainties in the estimation of the baseline and I_0 as well as uncertainties in the fitting. The obtained result is in excellent agreement with the known pressure of (1.61 ± 0.01) mbar, determined using frequency-comb-based Fourier-transform spectroscopy. This demonstrates that the pyroelectric receiver allows for accurate measurements and can be reliably used as detector for absorption spectroscopy measurements in the THz range.

In a previous work by Consolino et al. [18], a comparable pyroelectric detector in a THz-QCL-based cryogen-free spectrometer was used but with a 3 dB bandwidth of only 30 Hz. The THz QCL was tuned in a similar fashion as was done in this study but with a tuning frequency that was too high for the detector's bandwidth, resulting in the same type of deformations as we observed when using a bolometer as detector [15,16]. The PR No1 detector enables fast data acquisition and high sensitivity, and, in particular, its extraordinary bandwidth avoids any deformations of the absorption features.

Lastly, similar measurements were carried out with the pyroelectric receiver and the bolometer to investigate how the noise level of the pyroelectric receiver compared to that of the bolometer. To this end, absorption spectra similar to the one shown in Figure 6 were recorded for a variation of the total measurement time using laser tuning frequencies of 11 Hz and 201 Hz when measuring with the bolometer and the pyroelectric receiver, respectively. The total measurement time was given by the number of averages multiplied by the chopper frequency, i.e., half the laser tuning frequency, as the oscilloscope was triggered on the chopper signal. The measurements were performed in a comparable configuration, as illustrated in Figure 2a; however, no purging with nitrogen was performed, as the increase in the signal intensity would cause a saturation of the bolometer.

Figure 7 shows the standard deviation of the noise of the absorption spectra as a function of the total measurement time on a double logarithmic scale. For both the bolometer and the pyroelectric receiver, the results lie on a line with a slope of -0.5, as would be expected for shot-noise limited detection, implying that white noise is the dominating noise contribution for measurement times below 10 s. On these timescales, the SNR can be effectively improved by increasing the measurement time. The faster measurement rate possible with the pyroelectric receiver allows for a higher number of averages within the same measurement time, which compensates to some extent for its lower SNR. So, although single measurements performed with the pyroelectric receiver have an SNR that is worse by approximately a factor of 10 compared to the SNR of single measurements performed with the bolometer, the SNRs of absorption spectra recorded with the same measurement time differ by only a factor of 2. We note here that purging can additionally improve the SNR by a factor of 3 to 4, depending on the humidity level. Also a low-pass filter with a cut-off frequency of 10 kHz or smoothing filters could be used to digitally remove noise from the signal.

Based on the standard deviation of the noise given in Figure 7, the lowest detectable density of NH_3 can be calculated as the density that would correspond to an absorption profile with a peak value of three times the standard deviation of the noise. For example, for a total measurement time of 10 s, the resulting detection limits are 4×10^{14} cm^{-3} and 2×10^{14} cm^{-3}, corresponding to a pressure of 0.016 mbar and 0.008 mbar for the pyroelectric receiver and the bolometer, respectively. These values are valid for the used configuration only (see Figure 2a) and should be considered as rough estimates of the detection limits as the exact values depend on the humidity level, optical alignment, and other factors with an influence on the signal intensity.

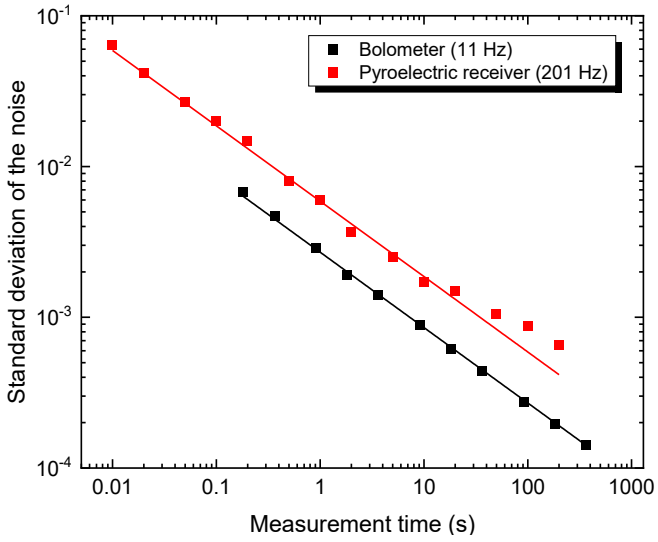

Figure 7. Standard deviation of the noise of absorption spectra recorded with the bolometer (at a tuning frequency of 11 Hz) and the pyroelectric receiver (at a tuning frequency of 201 Hz) as a function of the total measurement time.

4. Conclusions

This work introduced a new cryogen-free, high-speed pyroelectric receiver for absorption spectroscopy measurements in the THz range. To demonstrate its performance, absorption spectroscopy measurements were carried out on a reference gas cell with NH_3 using a tunable THz QCL at approximately 4.75 THz as the light source. Absorption spectra were successfully recorded without deforming the shape of absorption features for laser tuning frequencies up to 281 Hz. Measurements at higher tuning frequencies were possible as well, up to 1 kHz without deformations, but a faster optical chopper would be required to be able to quantitatively analyse the detected absorption spectra. A single absorption feature of NH_3 recorded using a tuning frequency of 201 Hz was analysed to determine the pressure inside the cell. The result was in excellent agreement with the pressure obtained with frequency-comb-based Fourier-transform spectroscopy. This demonstrates that the pyroelectric receiver can be reliably used as an alternative to helium-cooled bolometers for absorption spectroscopy measurements in the THz range, with its main advantages being the compactness, relatively low cost, and room-temperature operation.

Author Contributions: Conceptualisation, J.R.W., J.K. and J.-P.H.v.H.; methodology, J.R.W. and J.-P.H.v.H.; validation, J.R.W. and U.M.; formal analysis, J.R.W. and U.M.; investigation, J.R.W. and U.M.; resources, X.L., L.S., M.B., J.K. and J.-P.H.v.H.; data curation, J.R.W.; writing—original draft preparation, J.R.W., M.B., J.K. and J.-P.H.v.H.; writing—review and editing, all authors; visualisation, M.B., J.K. and J.R.W.; supervision, K.-D.W. and J.-P.H.v.H.; project administration, J.-P.H.v.H.; funding acquisition, L.S. and J.-P.H.v.H. All authors have read and agreed to the published version of the manuscript.

Funding: This research was funded by the Leibniz Gemeinschaft (grant no. K54/2017).

Data Availability Statement: The data presented in this study are available on request from the corresponding author due to privacy.

Acknowledgments: The authors would like to thank K. Biermann, B. Röben, W. Anders, C. Herrmann, A. Riedel, A. Tahraoui, and especially H. T. Grahn (all PDI) for their valuable contributions to fabricating the used THz QCL, F. Weichbrodt (INP) for the technical support, and I. Sadiek (INP) for performing the frequency-comb-based Fourier-transform spectroscopy measurements.

Conflicts of Interest: Author Matthias Budden was employed by the company WiredSense GmbH. Author Johannes Kunsch was employed by the company Laser Components Germany GmbH. The

remaining authors declare that the research was conducted in the absence of any commercial or financial relationships that could be construed as a potential conflict of interest.

References

1. Leitenstorfer, A.; Moskalenko, A.S.; Kampfrath, T.; Kono, J.; Castro-Camus, E.; Peng, K.; Qureshi, N.; Turchinovich, D.; Tanaka, K.; Markelz, A.G.; et al. The 2023 terahertz science and technology roadmap. *J. Phys. D Appl. Phys.* **2023**, *56*, 223001. [CrossRef]
2. Dhillon, S.S.; Vitiello, M.S.; Linfield, E.H.; Davies, A.G.; Hoffmann, M.C.; Booske, J.; Paoloni, C.; Gensch, M.; Weightman, P.; Williams, G.P.; et al. The 2017 terahertz science and technology roadmap. *J. Phys. D Appl. Phys.* **2017**, *50*, 043001. [CrossRef]
3. Vitiello, M.S.; Scalari, G.; Williams, B.S.; De Natale, P. Quantum cascade lasers: 20 years of challenges. *Opt. Express* **2015**, *23*, 5167–5182. [CrossRef] [PubMed]
4. Köhler, R.; Tredicucci, A.; Beltram, F.; Beere, H.E.; Linfield, E.H.; Davies, A.G.; Ritchie, D.A.; Iotti, R.C.; Rossi, F. Terahertz semiconductor-heterostructure laser. *Nature* **2002**, *417*, 156–159. [CrossRef] [PubMed]
5. Williams, B.S. Terahertz quantum-cascade lasers. *Nat. Photonics* **2007**, *1*, 517–525. [CrossRef]
6. Gao, L.; Feng, C.; Zhao, X. Recent developments in terahertz quantum cascade lasers for practical applications. *Nanotechnol. Rev.* **2023**, *12*, 20230115. [CrossRef]
7. Lü, X.; Röben, B.; Biermann, K.; Wubs, J.R.; Macherius, U.; Weltmann, K.D.; van Helden, J.H.; Schrottke, L.; Grahn, H.T. Terahertz quantum cascade lasers for high-resolution absorption spectroscopy of atoms and ions in plasmas. *Semicond. Sci. Technol.* **2023**, *38*, 035003. [CrossRef]
8. Hagelschuer, T.; Rothbart, N.; Richter, H.; Wienold, M.; Schrottke, L.; Grahn, H.T.; Hübers, H.W. High-spectral-resolution terahertz imaging with a quantum-cascade laser. *Opt. Express* **2016**, *24*, 13839–13849. [CrossRef] [PubMed]
9. Perraud, J.B.; Chopard, A.; Guillet, J.P.; Gellie, P.; Vuillot, A.; Mounaix, P. A Versatile Illumination System for Real-Time Terahertz Imaging. *Sensors* **2020**, *20*, 3993. [CrossRef]
10. Naftaly, M.; Vieweg, N.; Deninger, A. Industrial Applications of Terahertz Sensing: State of Play. *Sensors* **2019**, *19*, 4203. [CrossRef]
11. Giordano, M.C.; Mastel, S.; Liewald, C.; Columbo, L.L.; Brambilla, M.; Viti, L.; Politano, A.; Zhang, K.; Li, L.; Davies, A.G.; et al. Phase-resolved terahertz self-detection near-field microscopy. *Opt. Express* **2018**, *26*, 18423–18435. [CrossRef] [PubMed]
12. Rezac, L.; Hartogh, P.; Guesten, R.; Wiesemeyer, H.; Hübers, H.W.; Jarchow, C.; Richter, H.; Klein, B.; Honingh, N. First detection of the 63 µm atomic oxygen line in the thermosphere of Mars with GREAT/SOFIA. *Astron. Astrophys.* **2015**, *580*, L10. [CrossRef]
13. Richter, H.; Buchbender, C.; Guesten, R.; Higgins, R.; Klein, B.; Stutzki, J.; Wiesemeyer, H.; Hübers, H.W. Direct measurements of atomic oxygen in the mesosphere and lower thermosphere using terahertz heterodyne spectroscopy. *Commun. Earth Environ.* **2021**, *2*, 19. [CrossRef]
14. Hübers, H.W.; Richter, H.; Graf, U.U.; Guesten, R.; Klein, B.; Stutzki, J.; Wiesemeyer, H. Direct detection of atomic oxygen on the dayside and nightside of Venus. *Nat. Commun.* **2023**, *14*, 6812. [CrossRef]
15. Wubs, J.R.; Macherius, U.; Weltmann, K.D.; Lü, X.; Röben, B.; Biermann, K.; Schrottke, L.; Grahn, H.T.; van Helden, J.H. Terahertz absorption spectroscopy for measuring atomic oxygen densities in plasmas. *Plasma Sources Sci. Technol.* **2023**, *32*, 025006. [CrossRef]
16. Wubs, J.R.; Invernizzi, L.; Gazeli, K.; Macherius, U.; Lü, X.; Schrottke, L.; Lombardi, G.; Weltmann, K.D.; van Helden, J.H. Validation of THz absorption spectroscopy by a comparison with ps-TALIF measurements of atomic oxygen densities. *Appl. Phys. Lett.* **2023**, *123*, 081107. [CrossRef]
17. Lü, X.; Röben, B.; Pistore, V.; Biermann, K.; Luna, E.; Wienold, M.; Hübers, H.W.; Wubs, J.; van Helden, J.H.; Gellie, P.; et al. Terahertz quantum-cascade lasers: From design to applications. *IEEE Trans. Terahertz Sci. Technol.* **2024**. Submitted for publication.
18. Consolino, L.; Bartalini, S.; Beere, H.E.; Ritchie, D.A.; Vitiello, M.S.; Natale, P.D. THz QCL-based cryogen-free spectrometer for in situ trace gas sensing. *Sensors* **2013**, *13*, 3331–3340. [CrossRef] [PubMed]
19. Hübers, H.W.; Pavlov, S.G.; Richter, H.; Semenov, A.D.; Mahler, L.; Tredicucci, A.; Beere, H.E.; Ritchie, D.A. High-resolution gas phase spectroscopy with a distributed feedback terahertz quantum cascade laser. *Appl. Phys. Lett.* **2006**, *89*, 061115. [CrossRef]
20. Hübers, H.W.; Richter, H.; Wienold, M. High-resolution terahertz spectroscopy with quantum-cascade lasers. *J. Appl. Phys.* **2019**, *125*, 151401. [CrossRef]
21. Hagelschuer, T.; Wienold, M.; Richter, H.; Schrottke, L.; Grahn, H.T.; Hübers, H.W. Real-time gas sensing based on optical feedback in a terahertz quantum-cascade laser. *Opt. Express* **2017**, *25*, 30203–30213. [CrossRef]
22. Theocharous, E. Absolute linearity measurements on a gold-black-coated deuterated L-alanine-doped triglycine sulfate pyroelectric detector. *Appl. Opt.* **2008**, *47*, 3731–3736. [CrossRef] [PubMed]
23. Whatmore, R.W.; Ward, S.J. Pyroelectric infrared detectors and materials—A critical perspective. *J. Appl. Phys.* **2023**, *133*, 080902. [CrossRef]
24. Dai, J.; Zhang, J.; Zhang, W.; Grischkowsky, D. Terahertz time-domain spectroscopy characterization of the far-infrared absorption and index of refraction of high-resistivity, float-zone silicon. *J. Opt. Soc. Am. B* **2004**, *21*, 1379–1386. [CrossRef]
25. Lang, N.; Puth, A.; Kowzan, G.; Hamann, S.; Röpcke, J.; Masłowski, P.; van Helden, J.H. Spectroscopic investigations of plasma nitrocarburizing processes with a mid-infrared frequency comb. In Proceedings of the High-Brightness Sources and Light-Driven Interactions, Strasbourg, France, 26–28 March 2018; Optica Publishing Group: Washington, DC, USA, 2018; p. MW4C.3. [CrossRef]

26. Endres, C.P.; Schlemmer, S.; Schilke, P.; Stutzki, J.; Müller, H.S. The Cologne Database for Molecular Spectroscopy, CDMS, in the Virtual Atomic and Molecular Data Centre, VAMDC. *J. Mol. Spectrosc.* **2016**, *327*, 95–104. [CrossRef]
27. Gordon, I.E.; Rothman, L.S.; Hargreaves, R.J.; Hashemi, R.; Karlovets, E.V.; Skinner, F.M.; Conway, E.K.; Hill, C.; Kochanov, R.V.; Tan, Y.; et al. The HITRAN2020 molecular spectroscopic database. *J. Quant. Spectrosc. Radiat. Transf.* **2022**, *277*, 107949. [CrossRef]
28. Down, M.J.; Hill, C.; Yurchenko, S.N.; Tennyson, J.; Brown, L.R.; Kleiner, I. Re-analysis of ammonia spectra: Updating the HITRAN $^{14}NH_3$ database. *J. Quant. Spectrosc. Radiat. Transf.* **2013**, *130*, 260–272. [CrossRef]